

*APPARATUS FOR PRODUCTION OF A FREE PLASMA FILAMENT. DETERMINATION OF THE CURRENT AND RESISTANCE OF THE FILAMENT*

P. L. KAPITZA and S. I. FILIMONOV

Physics Laboratory, USSR Academy of Sciences

Submitted May 16, 1971

Zh. Eksp. Teor. Fiz. 61, 1016–1037 (September, 1971)

Part I. A description is given of an apparatus designed in the Physics Laboratory, Academy of Sciences, USSR, for production of a filamentary high-frequency plasma discharge freely floating in a resonator. The power supply is described. It consists of a 175 kW continuous-wave Nigotron generator which produces high-frequency oscillations of the  $H_{01}$  type of wavelength 19.4 cm. A device is described which transforms these operations into type  $E_{01}$ . The transformer is of the spider type; by rotating the legs of the spider it is possible to change the coupling of the generator with the resonator in which the discharge is produced. A description is given of the waveguide system which supplies the high-frequency power, and the design is described for the resonator in which the filament is produced. The equipment used for gas circulation, cooling, and initiation of the discharge is described.

Part II. A technique is described for studying a number of physical properties of the filamentary discharge. Methods are given for determination of the power absorption in the discharge, and for measurement of its length and of the high-frequency current in the filament. A technique and experiments are described for determining the absolute value of the high-frequency electric field in the resonator, and it is shown that the current in the filament is determined only by its reactance, which is mainly determined by the length of the filament. Measurements are presented of the current in a discharge in deuterium with an absorbed power up to 10 kW and for a length close to half the wavelength of the high-frequency field. This current is as much as 75 A. The resistive impedance of the filament is determined and the skin resistance is estimated. It is shown that for an ohmic resistance of the filament due to Coulomb scattering, this resistance corresponds to a hot plasma with an electron temperature close to a million degrees. It is also shown that for the high currents which exist in the plasma filament, a pinch occurs which can be balanced only by the pressure of the plasma in the hot state.

## INTRODUCTION

**I**N a previous article<sup>[1]</sup> we have reported the results of experimental studies of a freely suspended plasma filament produced in a resonator with high-frequency oscillations. On the basis of the results obtained, a theoretical analysis has been made which indicates that a region of hot plasma with an electron temperature of the order of 100 eV is produced inside the filament. The prospects for further study and practical application of the filamentary discharge are described in a second article.<sup>[2]</sup> The apparatus for obtaining this type of filamentary discharge and the measurement methods used in study of the plasma have been described only in general terms. Since the development of the apparatus and the methods of observation involves the solution of a number of technical problems which constitute the most time-consuming part of the work, we present in the present article a detailed description of the apparatus itself, in the first part, and, in the second part, of the experiments on determination of the size of the filamentary discharge and the power absorbed by it. In addition, we describe in detail the method for determining the value of the high-frequency current in the filament and its ohmic resistance, and report the latest experimental data.

## PART I. DESCRIPTION OF THE APPARATUS

### 1. High-Frequency Power Supply System

As has already been pointed out, the source of oscillations was a Nigotron—a generator of the magnetron type developed by us. The model which we used could provide continuous power up to 175 kW at a wavelength  $\lambda = 19.4$  cm. A detailed description of the design and operating characteristics of the Nigotron have been given previously.<sup>[3,4]</sup>

The entire apparatus and power supply are shown in Fig. 1. The Nigotron 1 (shown in outline) is placed in a resonator 3 which is surrounded by solenoid 2 which provides the magnetic field for the Nigotron. The solenoid is designed so that its inner shell is the vacuum shell of the Nigotron, which is connected to diffusion pumps 28. The Nigotron produces oscillations of type  $H_{01}$ , which must be converted to type  $E_{01}$  in order to maintain the longitudinal high-frequency current in the filament. The  $H_{01}$ - $E_{01}$  transformer is of the spider type, its design is shown in detail in Fig. 2. The principle on which it operates and the method for calculation of its design have been described previously.<sup>[5,6]</sup>

In our apparatus it is important that the coupling between the Nigotron and the working (load) resonator 6 be variable, depending on the amount of power fed to the filamentary discharge (see<sup>[1]</sup>, Sec. 5, p. 1842).

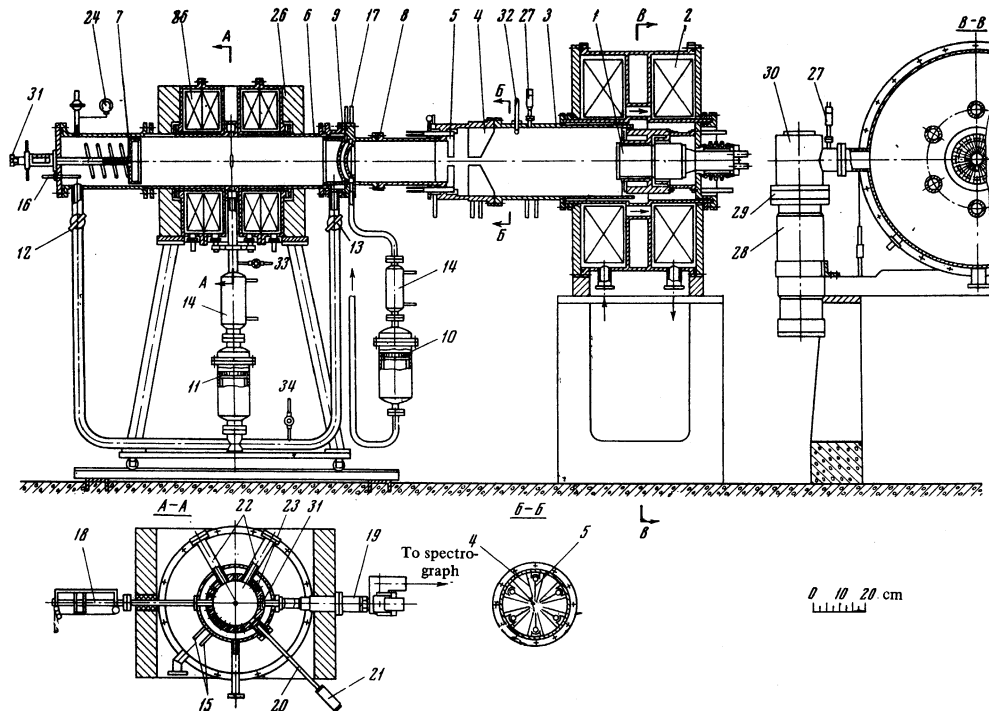


FIG. 1. Apparatus for study of the filamentary discharge: 1—Nigotron; 2—Nigotron solenoid; 3—Nigotron resonator; 4—grid which prevents penetration of  $E_{01}$  waves into the Nigotron resonator; 5—rotatable legs of the wave transformer; 6—body of load resonator; 7—resonator tuning plunger; 8—wave guide; 9—quartz window; 10—blower for cooling quartz window; 11—blower for circulation of gas in resonator; 12 and 13—valves for regulation of gas flow; 14—heat exchanger; 15—tubes carrying water to the load resonator; 16—tubes carrying water to the resonator tuning plunger; 17—tubes carrying water to the quartz window mounting; 18—lighter; 19—discharge image stabilizer; 20—endoscope; 21—vidicon; 22—supply tubes to the high-frequency circuit for excitation of magneto-acoustic oscillations in the filamentary discharge; 23—openings for outflow of gas; 24—valve for admission of gas and pressure gauge; 25—windings of solenoid for study of the effect of a magnetic field on the discharge; 26—solenoid yoke; 27—type LM-2 pressure gauges; 28—N-5 diffusion pump; 29—nitrogen trap; 30—type DU-160 vacuum valve; 31—quartz window; 32—measuring probe; 33 and 34—valves for connection of gas purification trap.

Since this coupling should be small, it turned out that it is quite adequate to make the legs 5 of the spider transformer straight and to change the amount of coupling by rotating them from a radial position by identical angles not greater than  $20^\circ$ . The coupling was determined experimentally as a function of the rotation angle of the legs by measuring the difference in the resonance frequencies  $\Delta\lambda_0$  corresponding to free oscillations of the resonator 6 (Fig. 1) for two positions of the plunger 7 separated by a distance  $\Delta L$ . The value of  $\Delta\lambda_0/\lambda_0$  is calculated with formula (5.2) of [1]. Figure 3 shows the experimentally measured values of  $\Delta\lambda_0/\lambda_0$  as a function of the rotation angle of the legs of the spider.

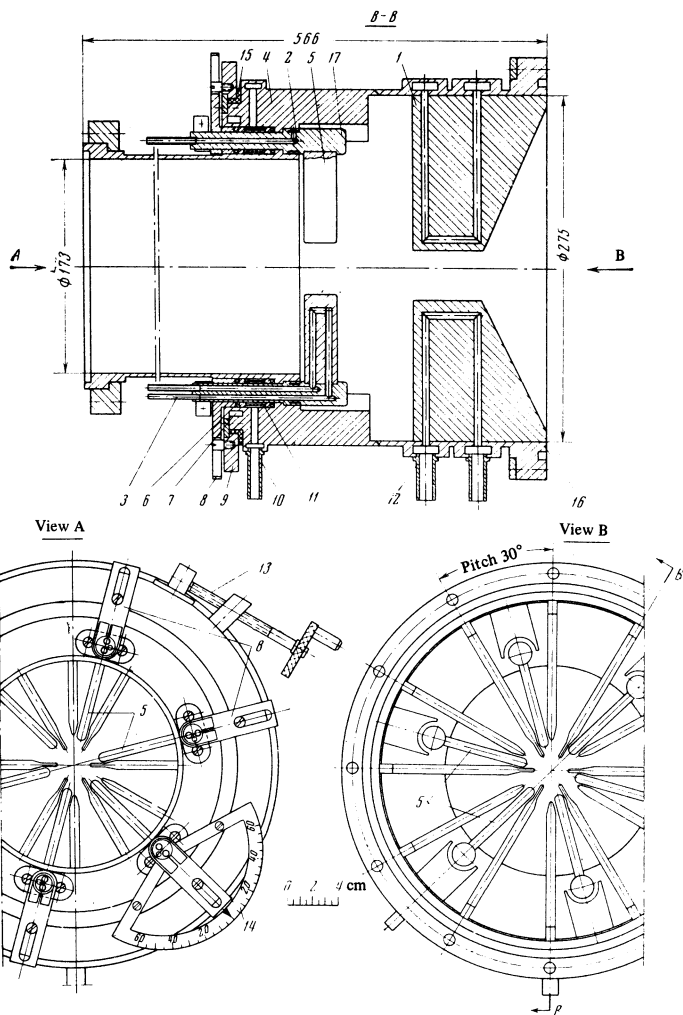
The design of the mechanism for rotating the legs is shown in Fig. 2, view A. Vacuum tightness of the apparatus during rotation of the spider legs is accomplished by a double system of Teflon gaskets 6, between which a fore vacuum is maintained. High conductivity for the high-frequency current between the legs and body of the spider is provided by hydraulic seals. In Fig. 2 it can be seen that the rods 17 which rotate the spider legs, where they enter the resonator body, have a ring-shaped channel 2 with a thin outer wall. This system is filled with oil and is connected by a small tube to a small piston pump with which the pressure on the oil can be raised to 30–50 atm. When this is done the outer wall of the channel is extended and forms a reliable contact with the main part of the apparatus. If these measures

are not taken to provide contact, at the high power levels with which we are dealing the rods will be welded to the body, and the spider legs will not rotate.

All parts of the wave transformer—the body, the spider legs, and the grid plates—are cooled by distilled water circulating in special channels, which in turn passes through a heat exchanger cooled by tap water. The Nigotron, the outer walls of the load resonator, and the waveguide (see Fig. 1) are also cooled by circulating distilled water. Each high-frequency element of the apparatus has its own cooling system, which is supplied with a flow meter and thermocouple. In this way we can trace the absorption of high-frequency power in the different parts of the apparatus independently.

Power was fed to the working resonator through a cylindrical waveguide 8 (Fig. 1) whose length was chosen so that its reactance would be small and the coupling with the working resonator would be high—in our case it was about 30%. This coupling is achieved through window 9 which consists of two disks of fused quartz. The quartz, which is of optical quality, has the shape of a convex meniscus of thickness 0.8 cm. The waveguide is under vacuum, and therefore the first disk is hermetically sealed with lead to a light copper ring in such a way that thermal expansion of the mounting cannot break the quartz. (We are indebted to Yu. V. Naïdich of the Institute for Study of Materials of the Ukrainian Academy of Sciences at Kiev for developing the technique

FIG. 2. Spider type transformer from  $H_{01}$  to  $E_{01}$  waves: 1—grid preventing penetration of  $E_{01}$  waves into Nigotron resonator; 2—hydraulic seal for transformer leg; 3—cooling water supply tube for rotatable leg; 4—transformer housing; 5—rotatable leg; 6—Teflon gasket; 7—water channel; 8—arm for rotation of leg; 9—ring for synchronous rotation of legs; 10—tubes for connection of fore-vacuum pump; 11—spacer between Teflon gaskets; 12—cooling water supply tubes for grid 1; 13—mechanism for rotation of ring 9; 14—leg rotation indicator; 15—bearing for ring 9 (textolite); 16—copper spacer for high-frequency seal; 17—rods for rotation of legs.



of soldering to quartz.) A second quartz meniscus is located 1 cm from the first in the resonator. The gap between the disks is necessary so that gas can be flowed through it and provide cooling for the quartz windows. The second meniscus does not need to be sealed very well.

At the high power levels which must be used, development of a system for supplying high-frequency power to the filament is a major problem. For example, if the vacuum in the Nigotron deteriorates and a low level of luminescence occurs at the quartz window, the quartz will rapidly become cloudy at various points, these regions begin to heat, and this leads to cracking of the quartz.

The vacuum in the Nigotron and the waveguide is maintained by two oil diffusion pumps 28 with a speed of 500 liters per second. Pumping is accomplished through traps cooled by liquid nitrogen.

2. Load Resonator

The design of the resonator which was used to study the discharge without a magnetic field is shown in detail in Fig. 4. In this resonator the discharge is more accessible for study.

Figure 1 shows the design of the resonator 6 in which the effect of a magnetic field on the discharge was stud-

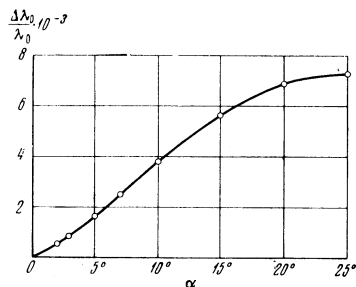


FIG. 3. Value of  $\Delta\lambda_0/\lambda_0$  as a function of rotation angle of the legs of the  $H_{01}$  to  $E_{01}$  transformer for  $\lambda = 19.31$  cm and a quartz window diameter of 120 mm.

ied. The magnetic field was obtained with a solenoid whose design is described in [7], except that we now obtained a magnetic field up to 25 kG with a uniformity along the axis of  $\pm 0.5\%$  in a length of 240 mm for an input power of 500 kW.

The resonator was tuned by moving plunger 7 by means of a screw. High-frequency contact between the plunger and the main part of the resonator is achieved by hydraulic seal 16, which consists of a thin-walled copper tube placed in a ring-shaped gap in the plunger. In the drawing (Fig. 4) it can be seen that the plunger has the shape of a cup made so that the point of contact

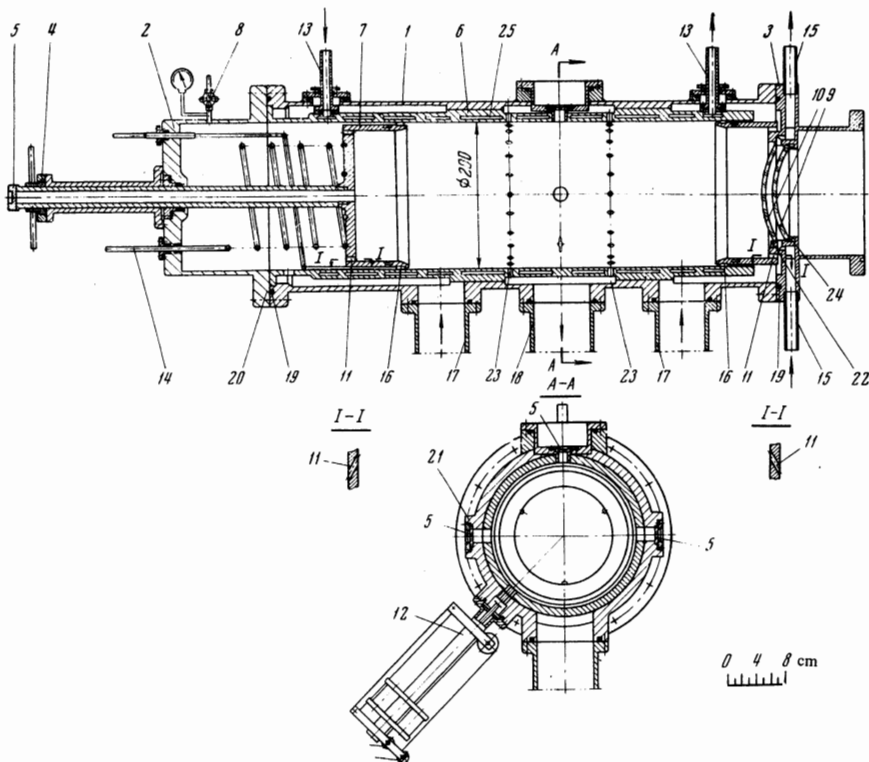


FIG. 4. Load resonator for study of the filamentary discharge: 1—outer body of resonator; 2—tuning plunger chamber; 3—quartz window holder; 4—screw and nut for movement of tuning plunger; 5—quartz windows; 6—internal resonator cylinder; 7—resonator tuning plunger; 8—valve for gas admission to resonator, and pressure gauge; 9—quartz window, soldered to frame 3; 10—cover quartz; 11—inclined nozzles; 12—device for initiation of discharge; 13—water cooling tubes to internal resonator cylinder 6; 14—water supply to resonator tuning plunger; 15—tubes for gas which cools the quartz window; 16—hydraulic seal; 17—tubes for supplying gas to nozzles 11; 18—tube for outflow of gas from resonator; 19—rubber gaskets; 20—copper gaskets; 21—indium gaskets; 22—quartz pins which hold the cover quartz; 23—openings for outflow of gas from the resonator; 24—water channel for quartz window; 25—water channels for resonator 6.

is located a quarter wavelength from the end of the plunger, since in this region the longitudinal currents in the resonator walls have their smallest value.

The resonator is assembled from a number of parts: the bottom, side windows, and so forth, and the joints must be tight both for filling with gas and for high-frequency currents. The first is accomplished by rubber gaskets, and the second either by hydraulic seals or by metallic gaskets of indium or copper wire.

The resonator (Fig. 4) has a number of side windows, both along the axis 5 (in an opening along the screw 4) and in the cylinder walls 6. Depending on the nature of the radiation to be studied, the windows were made of plastic, quartz, fluorite, and other materials. The size of the windows did not exceed 2.5 cm in diameter.

Rotation of the gas in the resonator, which is necessary for stabilization of the filament location, is accomplished by circulation of the gas by means of the inclined nozzles 11 located at the two ends of the resonator. The necessary outflow of gas occurs in the central cross section of the resonator through a number of small openings 23. Experiment shows that this system of circulating the gas gives the greatest stability in location of the discharge. Circulation of the gas was accomplished by a small blower (11 in Fig. 1). At first we used blowers from vacuum cleaners with commutator motors. Since the blower and motor were located in a region connected with the resonator for the sake of vacuum tightness, the carbon dust from the brushes, burning in the discharge, contaminated the gas. Therefore it was necessary to replace the vacuum-cleaner blowers with ones whose motors had no commutator. (The same blower serves for circulation of the gas between the quartz meniscuses located at the end of the waveguide—10 in Fig. 1.)

In the experiments on study of radiation in the ex-

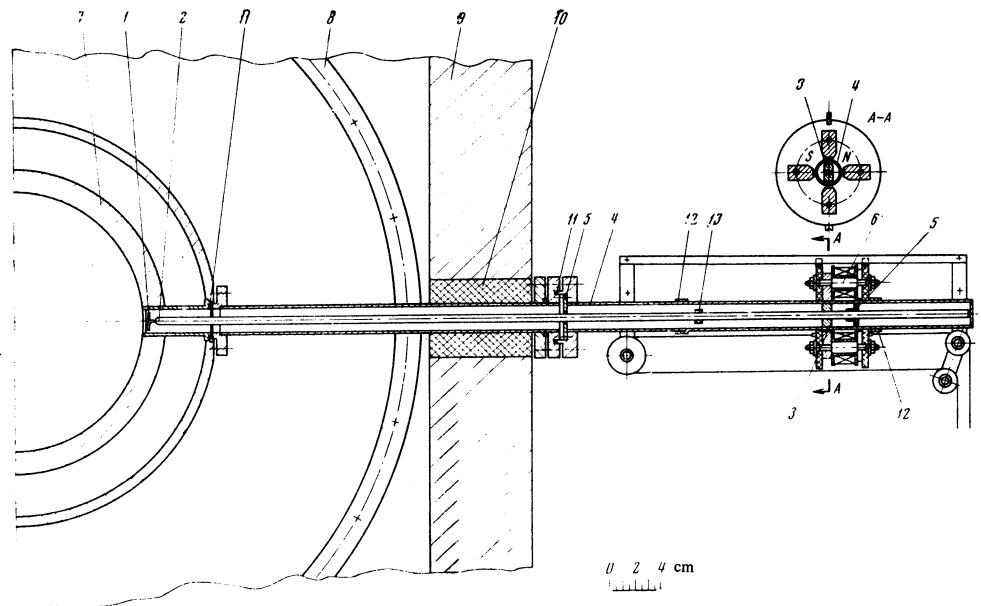
treme ultraviolet, very pure gas was necessary. By means of two valves 12 and 13 (Fig. 1) in the tubes conducting the gas to the nozzles, it was possible to establish the blast symmetrically, so that the filamentary discharge had no longitudinal motion. In carrying out these experiments we filled the resonator with especially pure deuterium, hydrogen, neon, or helium; these gases were continuously circulated through a trap filled with zeolite which was cooled by liquid nitrogen. Circulation was accomplished as the result of the pressure drop between points 33 and 34 (Fig. 1) in the manifold to which the tubes from the trap were connected.

The circulating gas was cooled by water as it passed through heat exchanger 14. The resonator walls and plunger were water cooled through channels 15–17, as is shown in the drawing. The body of the resonator and all of the fittings were made of mark M1 or MB copper.

### 3. Ignition of the Discharge

An essential part of the apparatus was the device for ignition of the discharge. We called it the "lighter" (Fig. 5). The function of the lighter was to place at the center of the resonator, where the discharge should ignite, a rod of length  $\sim 20$  mm made of tungsten wire 0.6 mm in diameter. This resulted in occurrence of the discharge at the correct place and at a reasonable intensity of the high-frequency oscillations. The ignition operation had to be performed rapidly, so that the tungsten would not melt. This is done as follows. The tungsten wire 1 (Fig. 5), fastened to the end of quartz rod 2 on which it is moved to the center of the resonator, is initially perpendicular to the resonator axis. In this position the high-frequency field does not act on the wire and it is not heated. Then the wire is rapidly turned through  $90^\circ$  and becomes parallel to the lines of

FIG. 5. Device for ignition of discharge (lighter): 1—tungsten wire; 2—quartz rod; 3—magnet; 4—housing with extension; 5—guides; 6—electromagnet; 7—load resonator; 8—jacket with solenoid winding; 9—solenoid yoke; 10—mounting sleeve; 11—rubber gaskets; 12—stops for motion of electromagnet; 13—stop for motion of quartz rod.



force, at which time corona discharges are formed at the ends of the wire which then ignite the discharge in the resonator. When this occurs, the wire is rapidly returned to its initial position and removed from the resonator. All of the manipulations are accomplished by means of the mechanism shown in Fig. 5. The quartz rod 2 is set into motion by means of a magnet 3 which is fastened to it, which moves in a hermetically sealed cylinder 4 where it can slide freely in the guides 5. An external electromagnet 6 which acts on magnet 3 is mounted on a quartz rod. It can be moved by remote control, moving the lighter into or out of the resonator. The electromagnet has two pairs of poles, which produce either a horizontal or a vertical field. By passing current through one and then through the other coil of the electromagnet, the lighter can be rotated rapidly. In spite of all the precautions, the tungsten wires still burned up after a hundred ignitions. We are currently developing an ignition system acting from the outside by means of the spark discharge of a high power laser.

#### 4. Conclusion

At the present time an apparatus is being developed with a discharge of large dimensions; it is similar to that described in this article, but differs in that the waveguide 8 (Fig. 1) with which power is fed to the resonator 6 is replaced by a coaxial line. Study of the filamentary discharge in this apparatus will permit us to check the correctness of the extrapolation of the results which we have obtained to filamentary discharges with higher powers.

We express our gratitude to our colleagues who have taken part in the development, preparation, and adjustment of this apparatus: designers A. I. Degal'tsev, Yu. E. Saprykin, A. D. Nikulin, and V. I. Tsvetkov; the mechanics in our shop where the apparatus was built, A. M. Goncharov, V. V. Khristyuk, and the late V. V. Aref'ev; and engineers V. I. Chekin and N. I. Kondrat'ev, who took part in adjustment of the apparatus.

## PART II. MEASUREMENT OF THE CURRENT AND RESISTANCE IN THE FILAMENT

### Introduction

The method of determining the high-frequency current in the filament has been described in Sec. 5 of <sup>[1]</sup>; in Fig. 5.2 of that article we have shown the results of current measurements for discharge powers up to 3.5 kW. At this power the filament length  $2l$  was significantly less than a half wavelength ( $2l \ll \lambda/2$ ) and it was not necessary to take into account the inductance of the filamentary discharge and the nonuniformity of the field in the resonator. In our further tests in which the filament power increased several times, in evaluation of the skin resistance we determined the current only approximately by linear extrapolation of the curve in Fig. 5.2 in <sup>[1]</sup> (see Sec. 6 in <sup>[1]</sup>, Eq. (6.16)).

In the present article we describe the determination of the power absorption in the discharge, and also the determination of the discharge dimensions. In addition we present the latest results on measurement of the current and resistance of the filamentary discharges for absorbed powers up to 10 kW for a filament length close to a half wavelength. These measurements were made by the same method described previously<sup>[1]</sup> but in contrast to the previous measurements we now take into account the inductance of the discharge and the nonuniformity of the field along the filament. Analysis of the results obtained in measurement of the current and resistance confirms that in the filament there is a region of hot plasma with an electron temperature estimated as in our earlier work<sup>[1]</sup> to be about  $10^6$  degrees.

### 1. Determination of the Power Absorbed by the Discharge

The power absorbed by the discharge is determined from the heating of the water which cools the jacket of the resonator 6, the plunger 7, and the heat exchangers 14 (Fig. 1). The water flow is measured by ordinary

flow meters. Since no special thermal insulation was used, heat exchange occurred with the external medium. A small amount of power was introduced also by the circulating motors 11 (Fig. 1).

In order to estimate the accuracy of the results obtained, we determined the influx of power from the surrounding medium and from the circulation motor in the absence of high-frequency oscillations, but with the circulation of gas. The value of this power was in the range 0.3–0.4 kW. Then we compared the power absorbed in the discharge for water flows differing by a factor of two. These measurements showed that the measured value of power absorbed by the discharge was somewhat exaggerated, but the error in its determination at 10 kW does not exceed 0.5 kW, which amounts to 5%, and at low powers the error does not exceed 10%. At this stage of the measurements this accuracy was sufficient for our purposes. The time required to establish the thermal conditions necessary for this measurement accuracy lay in the range 10–15 minutes. The power absorbed by the discharge was taken as one of the main characteristics of the discharge. It was studied as a function of pressure and gas composition. Some experimental data have already been presented in a previous article.<sup>[1]</sup>

**2. Determination of the Dimensions of the Filamentary Discharge**

The visible dimensions of the outline of the luminescence of the filament are characterized by a length  $2l$  and diameter  $2a_0$ . The length of the discharge was measured in the simplest possible way by means of a camera obscura with an objective aperture of 0.3 mm. By measuring the filament image on a ground glass with a bar gauge and knowing the distance from the objective to the filament and to the ground glass, it was possible to determine the filament dimensions rather reliably. The boundaries of the filament image on the ground glass of the camera obscura were defined with an accuracy of 1 mm for an image length of 50–90 mm, which allowed measurement with an accuracy of 2%.

The camera obscura could also be used to photograph the filament and determine its dimensions in this way. With an objective aperture of 0.3 mm and a film speed of 90 GOST units the exposure was  $\frac{1}{70}$  second. Experiments show that the filament length depends on the power input, composition and pressure of the gas, and the dc magnetic field. Measurements of the column length have been reported in <sup>[1]</sup>, Secs. 2 and 7. In order to show how strongly the gas composition affects the filament dimensions, we list below the values of power input  $P_a$  necessary to obtain a filamentary discharge of length 8 cm in deuterium-argon mixtures at pressures  $1.23 \text{ atm} < p < 1.63 \text{ atm}$ :

Gas composition	$P_a$ , kW
$D_2$	8.4
$D_2 + 12.4\% \text{ Ar}$	7.2
$D_2 + 26\% \text{ Ar}$	5.5
$D_2 + 38\% \text{ Ar}$	4.8
$D_2 + 50\% \text{ Ar}$	3.5

Subsequently it turned out to be convenient to follow the behavior of the filament continuously, observing its image on a television screen. This was accomplished by projection of the filament image through an endoscope onto a vidicon screen. By observing the behavior

of the discharge image on the screen, it is convenient to adjust the gas circulation so as to obtain the greatest stability.

As has already been described in <sup>[1]</sup>, Sec. 2, the cross section of the filament  $2a_0$  was determined from the intensity of luminescence; this was done in a stabilized image of the filament. A more detailed description of the stabilizer will be given in a subsequent article devoted to the methods of spectral investigation of the filamentary discharge.

Experiments showed that the visible dimensions of the luminous filament depend on the gas circulation, and therefore the filament dimensions determined as we have described give only an outline of the luminous cloud of the filament, and the dimensions of the internal plasma portion of the filament in which the high-frequency current flows were not obtained accurately; all we can say is that the size of the inner plasma region is smaller than the visible size.

From what follows it will be evident that, for a filament length close to  $\lambda/2$ , high accuracy is required in determination of the filament length. According to the picture adopted by us, the hot plasma is surrounded by a cloud of diameter  $2a_0$  which can lengthen the filament by this amount. Therefore the active length of the filament is

$$2l_0 = 2l - 2a_0, \tag{1}$$

where  $2a_0$  is the maximum visible size of the filament cross section calculated from Eq. (2.1) of <sup>[1]</sup>. In subsequent calculations we will use the value  $2l_0$  as the determined length of the filament. The data for deuterium have been given in <sup>[1]</sup> in Fig. 2.4.

**3. Absolute Measurement of the Field in the Resonator**

As has been described in Sec. 5 of <sup>[1]</sup>, in order to determine the current in the filament it is necessary to determine the absolute value of the electric field intensity  $\hat{E}_z$  on the axis of the load resonator in the absence of the filamentary discharge. This quantity is proportional to the high-frequency field  $\mathcal{E}$  in the Nigotron, and also depends on the coupling, which is determined by the rotation angle  $\alpha$  of the legs of the spider transformer (see Fig. 2).

The field  $\mathcal{E}$  in the Nigotron is measured by a loop with a thermocouple, which is placed in the Nigotron in such a way that it is threaded by the magnetic flux from type  $H_{01}$  oscillations. We note that if we determine the field  $\hat{E}_n$  for a thermocouple reading  $T_n$ , then for another reading  $T_0$  the field will be  $\hat{E}_0$ . Here

$$\hat{E}_0 = \hat{E}_n \sqrt{T_0 / T_n}. \tag{2}$$

The problem in the measurement is to determine the absolute value  $\hat{E}_n$  for some reading  $T_n$  of the thermocouple on the loop. We determined  $\hat{E}_n$  by measurement of the force exerted by the electric field on a conducting sphere suspended in the resonator. This method has been described by us previously.<sup>[8]</sup>

According to Eq. (4) of <sup>[8]</sup> the intensity of the high-frequency electric field at the resonator axis will be

$$\hat{E}_n = \sqrt{\frac{2\Lambda}{\pi r^3}} F_n, \tag{3}$$

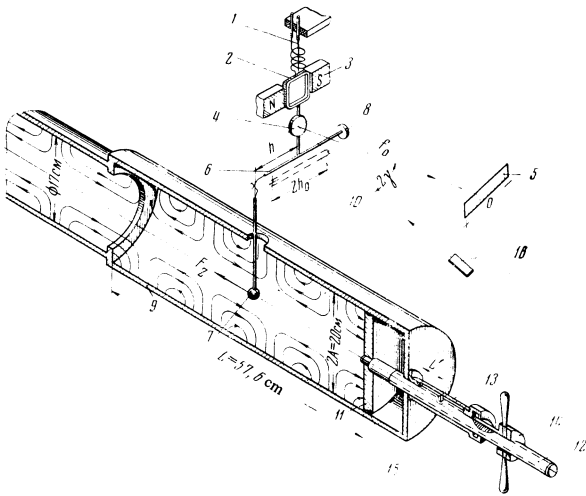


FIG. 6. Apparatus for measurement of the absolute field in the resonator: 1—beryllium bronze suspension; 2—frame with coil; 3—magnet; 4—mirror; 5—scale; 6—balance arm; 7—sphere. 8—load balancing the sphere; 9—body of load resonator; 10—rod added for calibration of suspension; 11—resonator tuning plunger; 12—screw; 13—scale for reading plunger motion (in millimeters), 14—nut which moves plunger, with vernier to 0.01 mm, 15—hydraulic seal.

where  $F_Z$  (in dynes) is the force due to the high-frequency field acting on this sphere,  $r$  is the radius of the sphere, and  $\Lambda$  is the guide wavelength in the resonator. In earlier work we measured the force  $F_Z$  from the deflection of the sphere, which was suspended by a thread as a pendulum. Although this method is simple, its sensitivity is low, an intense high-frequency field is required, and the sphere is heated substantially. Therefore in the present work we have measured the field  $F_Z$  by a torsion balance. This method is substantially more sensitive and gives more accurate results.

The measuring device is shown schematically in Fig. 6. The main suspension system was taken from an ordinary galvanometer. A frame 2 is hung on a beryllium bronze wire 1 of diameter  $8.5 \times 10^{-3}$  cm and length 2 cm. It moves in a gap in which a magnetic field is produced by a dc magnet 3. Below the frame is fastened a mirror 4, and at a distance  $f_0 = 121.2$  cm from it is located a transparent scale 5 for reading the motion of the light spot. Under the mirror is hung an arm 6, on one end of which a hollow silver sphere 7 of diameter  $2r = 1.514$  cm and weight 0.6 g is hung by a quartz fiber located a distance  $h$  from the support, and at the other end a counterweight 8. The sphere is located on the axis of the resonator 9 at the place where the force exerted on it by the high-frequency field has the greatest value. The measurement is made on the basis of the current  $j$  in the frame 2 which compensates the force on the sphere in such a way that the light spot on the scale remains at zero.

The deflection of the light spot on the scale,  $y$ , obviously will be proportional to the current  $j$ :

$$y = Bj. \quad (4)$$

If the rotation angle is denoted by  $\gamma$ , the oscillation of the system is determined by the equation

$$hF_z = J\ddot{\gamma} + K_0\dot{\gamma}. \quad (5)$$

where  $J$  is the moment of inertia of the system. The angle  $\gamma$  is determined from the deflection of the light spot:

$$\gamma = \frac{1}{2}y / f_0. \quad (6)$$

The constant  $K_0$  is determined in the usual way from the two periods of free oscillation. The first,  $t_1$ , is for free oscillation of the system; then we have

$$F_z = 0, \quad K_0 = J(2\pi / t_1)^2. \quad (7)$$

The second period,  $t_2$ , is for the case when the arm is subjected to an additional load 10, shown in Fig. 6 by dashed lines, which consisted of a lead cylinder of length  $2h_0$  with a moment of inertia  $J_0 = \frac{1}{3}mh_0^2$ . Then

$$F_z = 0, \quad K_0 = (J + J_0)(2\pi / t_2)^2. \quad (8)$$

From these two expressions we obtain

$$K_0 = J_0 \frac{(2\pi)^2}{t_2^2 - t_1^2}. \quad (9)$$

Thus, the force  $F_Z$  is determined from Eqs. (4)–(6) and we obtain

$$\gamma = 0, \quad F_z = \frac{K_0 B}{2hf_0} j. \quad (10)$$

In our apparatus,  $m = 7.113$  g,  $h = 3.18$  cm,  $h_0 = 2.5$  cm,  $J_0 = 14.82$  g-cm<sup>2</sup>,  $t_1 = 2.24$  sec, and  $t_2 = 2.98$  sec. Hence from (9) we find  $K_0 = 1.54 \times 10^2$ .

The coefficient  $B$  is determined experimentally from the deflection of the light spot. From experiment  $y = 5.25$  cm for  $j = 32.95$   $\mu$ A, and hence from Eq. (4) we have  $B = 0.159$  cm/ $\mu$ A.

Finally from Eq. (10) we obtain

$$F_z = 3.17 \cdot 10^{-2} j \text{ [dynes]}, \quad (11)$$

where  $j$  is measured in  $\mu$ A.

From Eqs. (3) and (11) for  $2r = 1.514$  cm and  $\Lambda = 28.8$  cm, we find for the field in the resonator for a compensating current  $j$

$$E_n = 1.16 \sqrt{j} \text{ [e.s.u.].} \quad (12)$$

The intensity of the high-frequency field in the Nigotron, as we have already indicated, is determined from the reading  $T$  of the loop thermocouple, whose design is shown in Fig. 7. The thermocouple loop 1 consists of constantan and copper wires of diameter 0.06 mm and length 6 mm each. The wires are welded together at one end, and the free end of the constantan wire is soldered to a copper rod 2 of diameter 1.2 mm which is placed in a copper cylinder 3. At the end of the cylinder there is a fitting in the form of a tube 4 of small diameter; the free end of the copper wire of the thermocouple loop is soldered to this fitting. The gap between the rod 2 and tube 4 is filled with BF glue, which assures a constant temperature of the contacts at the other end of the constantan-copper pair. Since the loop is located in vacuum, vacuum tightness of the system is provided by bringing the copper rod 2 out through an insulating glass bead 5. The thermocouple can be moved into the Nigotron resonator by means of a threaded head 6 which compresses the sylphon bellows 7. The thermocouple had a resistance of about 3 ohms and was usually placed at the depth in the Nigotron at which the emf  $T$  was about 1 mV under working conditions. Control

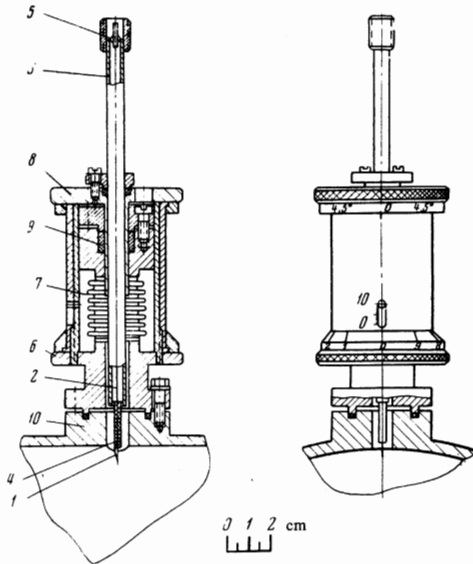


FIG. 7. Design of thermocouple loop: 1—copper-constantan thermocouple loop; 2—copper rod; 3—support for copper loop; 4—copper tube; 5—glass bead insulator; 6—nut controlling depth of penetration of loop in Nigotron resonator; 7—syphon bellows; 8—flange for rotation of loop in resonator; 9—Teflon packing box, 10—Nigotron resonator wall.

Table I

$L'$ , cm	$j$ , $\mu A$	$T_n$ , mV	$\hat{E}_0$ , e.s.u.	$\lambda$ , cm
5.9	12.4	0.92	4.22	19.4278
5.8	14.5	0.92	4.61	19.4271
5.6	21.4	0.91	5.62	19.4258
5.4	33.6	0.90	7.08	19.4231
5.3	43.0	0.88	8.11	19.4216

For  $\alpha = 8.5^\circ$ ,  $T_0 = 1$  mV.

measurements showed that, in spite of the simplicity of the design, the accuracy of measurements of  $T$  with the thermocouple was about 1% with good stability.

Measurements of  $\hat{E}_n$  were made for different couplings between the Nigotron and the resonator, determined by the rotation angle  $\alpha$  of the legs of the  $H_{01}-E_{01}$  spider transformer. Here the measurements were made for different positions of the plunger 11 (Fig. 6), which changed the length of the resonator cavity. Movement of the plunger 11 was accomplished by the screw 12. The amount of motion was determined from reading scale 13 and from the rotation of the nut 14 on the screw, with an accuracy of 0.01 mm. The plunger location  $L'$  was determined with reference to an arbitrary point on the scale. The wavelength  $\lambda$  was determined with a heterodyne frequency meter type GCh-1M with an accuracy to six decimal places.

An example of the measured values for a coupling corresponding to  $\alpha = 8.5^\circ$  is given in Table I, where we have shown the values of  $\hat{E}_0$  (in electrostatic units) obtained by reduction of  $\hat{E}_n$  according to Eq. (2) to the same field intensity in the Nigotron corresponding to a thermocouple reading  $T_0 = 1$  mV.

The accuracy in measurement of the value of  $\hat{E}_0$  was particularly studied. The size of the sphere and its location in the resonator were varied, measurements were made on both sides of resonance, and so forth. We consider that the accuracy in determination of the absolute value of  $\hat{E}_0$  is no better than 4%, and the accuracy in the

relative values substantially better—about 1%, and repeated measurements agreed within this accuracy.

Once the absolute value of the amplitude  $\hat{E}_0$  on the resonator axis has been determined, it is possible to find from Eqs. (5.14) of [1] the quantity  $\beta\mathcal{E}$ —the strength of the forcing oscillations. In the absence of a discharge, assuming a high value of  $Q$  for the working resonator, we have

$$D_e(1 - \omega^2 / \Omega_0^2)\hat{E}_0 = \beta\mathcal{E}. \quad (13)$$

Here  $D_e$ —a coefficient in the expression for the energy of the electric field of the resonator—is calculated according to Eq. (5.9) of [1] from the resonator dimensions, and  $\Omega_0$  is the natural frequency of the resonator. The principal difficulty in using Eq. (13) lies in accurate determination of the quantity in parentheses, since this is the difference of two nearly equal quantities, and in order to determine the ratio  $\omega^2 / \Omega_0^2$  it is necessary to know accurately the degree of detuning of the resonator. This difficulty can be overcome if we determine two values  $\hat{E}'_0$  and  $\hat{E}''_0$  for two positions of the plunger in the resonator far from resonance (at a distance  $\Delta L$ ) and for the same thermocouple reading  $T_0$  in the Nigotron. Then by algebraic transformations we obtain Eq. (5.17) of [1], which we give in somewhat different form, with inclusion of a change in the thermocouple readings  $T$ :

$$\beta\mathcal{E} = 2D_e \frac{\hat{E}'_0\hat{E}''_0 - \hat{E}_0^2}{\hat{E}''_0 - \hat{E}'_0} \frac{\Delta\lambda_0 + \Delta\lambda}{\lambda_0} \sqrt{\frac{T}{T_0}} \equiv \beta\bar{\mathcal{E}} \sqrt{\frac{T}{T_0}}. \quad (14)$$

The quantity  $D_e$  characterizing the resonator is calculated from Eqs. (5.9) and (5.1) of [1], where  $\lambda_0 = 19.4$  cm,  $\Lambda = 28.8$  cm,  $L = 57.6$  cm,  $A = 10$  cm (see Fig. 6), and

$$J_1\left(\frac{2\pi}{\lambda_c} A\right) = 0.519.$$

As a result we obtain  $D_e = 3.5 \times 10^2$  cm<sup>3</sup>.

The frequency shift on movement of the resonator plunger is given by Eq. (5.2) of [1] ( $n = 4$ , see Fig. 6) as

$$\Delta\lambda_0 = \frac{2\Delta L}{n} \left(\frac{\lambda_0}{\Lambda}\right)^3 = 0.153 \Delta L. \quad (15)$$

The change in frequency of oscillations produced by retuning of the resonator is determined directly from the wave meter and, according to Eq. (5.19) of [1], will be

$$\Delta\lambda = \lambda' - \lambda''. \quad (16)$$

As an example, for the data listed in Table I, for a retuning  $\Delta L = 5.9 - 5.3 = 0.6$  cm from (15) and (16) we have  $\Delta\lambda_0 = 9.18 \times 10^{-2}$  cm and  $\Delta\lambda = -0.62 \times 10^{-2}$  cm. Then in determination of the quantity  $\beta\mathcal{E}$  from Eq. (14) we obtain for  $\alpha = 8.5^\circ$  and  $T_0 = 1$  mV

$$\beta\mathcal{E} = 27.2\sqrt{T} \text{ [ a.e.s.u. ]}.$$

The results calculated for other couplings are given in Table II.

The method described for determination of  $\beta\mathcal{E}$  has the further advantage that it excludes the effect of the waveguide 8 which connects the converter 5 with the resonator 6; see Fig. 1. This exclusion would be complete if in movement of the plunger no change in wavelength  $\Delta\lambda$  occurred (see (16)). This effect turns out to be small; calculations show that the corresponding error is less than 1.5%.

Table II

$P_a$ , kW	$l$ , cm	$2a_0$ , cm	$2a_0$ , cm	$l_0 = -a_0$ , cm	$T$ , mV	$\alpha$ , deg	$\beta$ , deg	$\beta_{\text{eff}}$ , e.s.u.	$f(\xi)$	$l_0 \left[ 1 - \left( \frac{4l_0}{\lambda} \right)^2 \right]$	$\hat{I}_0$	$R$ , ohms	$\rho_m$ , ohms	$Z_r$ , ohms	$Z_a$ , ohms
5.0	3.2	0.16	0.23	3.1	1.0	4.0	12.2	0.867	1.83	18.7	29	5.7	74	6.2	
6.0	3.5	0.2	0.28	3.4	1.05	4.5	13.0	0.841	1.73	22.3	24.3	5.6	54	5.0	
8.0	4.1	0.3	0.42	3.9	0.82	6.5	19.9	0.793	1.38	40.0	10	2.9	26	1.7	
10.0	4.5	0.4	0.57	4.2	0.81	8.5	27.2	0.761	1.05	75.0	3.6	1.3	14	0.6	

For  $\Lambda = 28.8$  cm,  $\lambda = 19.4$  cm,  $p_0 = 1$  atm of deuterium.

#### 4. Measurement of the High-Frequency Current in the Filament

We showed previously<sup>[1]</sup> that if we have determined the field strength  $E_Z$  we can find the amplitude  $\hat{I}_0$  of the current which flows in the central cross section of the filament. As we will show, the value of this current does not depend on the skin resistance, but is determined only by the filament shape, and therefore these measurements have good reliability.

The method of determining the current  $\hat{I}_0$  is based on the second expression (5.14) of<sup>[1]</sup>. While a discharge is present the resonator is tuned close to resonance, and since its  $Q$  is high the term in square brackets can be set equal to zero. For small filaments when  $2l_0 \ll \lambda/2$ , it was necessary in<sup>[1]</sup> to take into account only the electrostatic interaction (the coefficient  $M_e$ ) of the filament with the field in the resonator, and in that case Eq. (5.19) of<sup>[1]</sup> was available for determination of the current.

For powerful discharges where  $2l_0 \sim \lambda/2$ , it is necessary to take into account the magnetic interaction (the coefficient  $M_m$ ), and the current is determined by the following expression:

$$\hat{I}_0 = \frac{\omega \beta \tilde{\mathcal{E}} \sqrt{T}}{M_e - \omega^2 M_m} \quad \text{for } T_0 = 1 \text{ mV.} \quad (17)$$

The coefficient  $M_e$  is determined as before from the electrical interaction energy between the filament and the resonator field on the basis of Eq. (5.11) of<sup>[1]</sup>. In making this calculation for filaments with a length close to  $\Lambda/2$  — a half wavelength in the resonator — it is also necessary to take into account the sinusoidal nature of the field  $E_Z$  along the  $z$  axis (see Eq. (5.3) of<sup>[1]</sup>). Then, instead of Eq. (5.12) of<sup>[1]</sup> which determines  $M_e$  for  $\Lambda \gg 2l$ , we will have

$$M_e q_0 = \int_{-l_0}^{l_0} \delta z \cos \frac{2\pi}{\Lambda} z dz, \quad (18)$$

where  $l_0$  is the actual filament length determined by Eq. (1), and  $q_0$  is the quantity of charge flowing through the central cross section of the filament.

We assume the distribution of linear surface charge density  $\delta$  to be the same as that given by (5.22) of<sup>[1]</sup>. Using Eq. (5.23) for  $q_0$  and including (5.24)<sup>[1]</sup>, we obtain

$$M_e = \frac{2}{l_0^2} \int_{-l_0}^{l_0} z^2 \cos \frac{2\pi}{\Lambda} z dz. \quad (19)$$

Carrying out the integration in (19) and defining

$$\xi = 2\pi l_0 / \Lambda, \quad (20)$$

we have

$$M_e = 4l_0 \left[ \frac{2}{\xi^2} \cos \xi + \left( \frac{1}{\xi} - \frac{2}{\xi^3} \right) \sin \xi \right]. \quad (21)$$

For calculations in which  $\xi$  is close to unity, it is

convenient to reduce this expression to the following form:

$$M_e = {}_4/3 l_0 f(\xi), \quad (21')$$

where

$$f(\xi) = \frac{\sin \xi}{\xi} \left[ 1 - \frac{2\xi^2}{15} - \frac{4\xi^4}{315} - \dots \right]. \quad (22)$$

The difficulty in determination of the coefficient  $M_m$  for the magnetic interaction between the resonator and the filament is due to the absence of theoretical calculations, which evidently involve substantial complications. On the basis of general considerations, we take the coefficient  $M_m$  as equal to  $M_e$  times the square of the ratio of the field frequency to the natural resonant frequency of the filament<sup>1)</sup> (see also<sup>[1]</sup>, p. 1840). The validity of the expression which we used for  $M_m$  was checked as follows.

As is well known,<sup>[9]</sup> the resonant wavelength for an ellipsoid of revolution with semiaxes  $b$  (small) and  $l_0$  (large) is

$$\lambda_p = 4l_0(1 + \sigma), \quad (23)$$

where

$$\sigma = 0.35 / \left( \ln \frac{2l_0}{b} \right)^2 \quad \text{for } b \ll l_0.$$

For our filamentary discharges it can be assumed with an accuracy of 2–3% that the resonant half wavelength  $\lambda_p/2$  is equal to the filament length  $2l_0$ . In order to determine the validity of this assumption, we constructed a model in which, instead of the filamentary discharge, we placed in the resonator an ellipsoid turned from copper, and measured the resonant wavelength of this system. The equations (5.14)<sup>[1]</sup> were solved for  $E_0$  and  $q_0$  on the assumption  $\beta = 0$ . We obtained an equation for determination of the resonant frequency  $\omega_r$  and the wavelength  $\lambda_r$  corresponding to it for the system being studied:

$$(M_e - \omega^2 M_m)^2 - \frac{D_e}{c_p} \left[ 1 - \left( \frac{\omega_r}{\Omega_0} \right)^2 \right] \left[ 1 - \left( \frac{\omega_r}{\Omega_p} \right)^2 \right] = 0. \quad (24)$$

An experimental study of this model was made for us

<sup>1)</sup> An approximate calculation of the coefficient for magnetic interaction of the filamentary discharge with the high-frequency field of the resonator can be made as follows. According to Eq. (3.5) the magnetic field in the resonator near the filament will be

$$H_\phi = \frac{r\omega}{2c} E_0.$$

The magnetic field produced by the filament in this region is

$$H_\phi' = \frac{2}{rc} I.$$

According to (5.7) of ref. 1, the coefficient  $M_m$  is determined by the interaction energy of the magnetic fields  $H_\phi$  and  $H_\phi'$ . We will calculate it in a cylindrical volume of radius  $R$  and length  $2l_0$ . We have:

$$\omega^2 M_m = \frac{1}{4\pi E_0 q_0} \int_0^R \int_{-l_0}^{l_0} H_\phi H_\phi' \cdot 2\pi r dr dz.$$

by A. B. Manenkov, and it was shown that within the experimental accuracy of 2% its resonant wavelength  $\lambda_R$  agrees with  $\lambda_D$ , which is given by (23) as twice the ellipsoid length,  $4l_0$ .

In order to satisfy Eq. (24), the total interaction coefficient of the resonator and filament must within the necessary accuracy be equal to

$$M_e - \omega^2 M_m = M_e \left[ 1 - \left( \frac{4l_0}{\lambda} \right)^2 \right]. \quad (25)$$

In this case Eq. (17) for determination of the current, with incorporation of (22) and (25), takes the form

$$\hat{I}_0 = \frac{3}{4} \frac{\omega \beta \mathcal{E} \sqrt{T}}{l_0 [1 - (4l_0/\lambda)^2] f(\xi)} \quad (T_0 = 1 \text{ mV}). \quad (26)$$

Converting to amperes and wavelengths, we have

$$\hat{I}_0 = \frac{15\pi}{\lambda} \frac{\beta \mathcal{E} \sqrt{T}}{l_0 [1 - (4l_0/\lambda)^2] f(\xi)} [a]. \quad (27)$$

The experimental data necessary for calculation of the current for various powers are given in Table II. We have listed the power  $P_a$ , the thermocouple reading  $T$ , the angle  $\alpha$  and the filament dimensions  $2l_0$  and  $2a_0$  corresponding to it, taken from the curves in Figs. 2.5 and 2.4 of <sup>[1]</sup>, and also the calculated values of  $f(\xi)$  and the current  $\hat{I}_0$ .

We will analyze the main factors affecting the accuracy of the current determination. The principal factor is the error in determination of the filament length  $2l_0$ , since the estimate of the effect of the cloud according to Eq. (1) is apparently somewhat arbitrary and is likely to give too small a value for the length  $2l_0$ , which reduces the calculated current. This shows up appreciably only for high power  $P_a$ , but even in that case the error in current determination is apparently no more than 5–10%. The error in determination of the absolute value of  $\beta \mathcal{E}$  is estimated by us as 5%.

As we have already pointed out, the validity of Eq. (17) for determination of the current, which was obtained from Eqs. (5.14) of <sup>[1]</sup>, depends on how close the resonator is to resonance. Near resonance the term with  $D_e$  becomes small and does not affect the determination of the current in the filament. The validity of this condition was checked experimentally—for a constant power in the filament the resonator plunger was moved from the resonance position by a distance two to three times greater than occurred in the measurements. The experiments showed that the displacement of the plunger did not have an appreciable effect.

On comparing the previous measurements shown in

Using Eqs. (5.5), (5.26), and (5.29) from ref. 1, and also (21'), after integration we obtain

$$\omega^2 M_m = \left( \frac{\pi R}{\lambda} \right)^2 M_e.$$

The integration limit  $R$  is determined mainly by the configuration of the field  $H'_\varphi$  near the filament, and therefore  $R$  is smaller than the resonator radius  $A$  and can be assumed proportional to the filament length  $2l_0$ .

If we assume  $R = 4l_0/\pi$ , we obtain the expression adopted by us for the interaction coefficient of the filament with the resonator field:

$$M = M_e \left[ 1 - \left( \frac{4l_0}{\lambda} \right)^2 \right], \quad l_0 < A.$$

Fig. 5.2 in <sup>[1]</sup> with the present measurements and taking into account the fact that the previous measurements were made less carefully, we can conclude that the agreement is quite satisfactory.

## 5. Determination of Filament Resistance

According to Eq. (5.28) of <sup>[1]</sup>, the filament resistance  $R$  is

$$R = 2F_a / I_0^2. \quad (28)$$

The accuracy in determination of  $R$  is limited by the accuracy in determination of the power  $P_a$ . The power measurement was described in Sec. 1, and we consider the values obtained to be exaggerated but not by more than 5–10%.

We noted at the beginning of Sec. 4 that in our calculations we have assumed that the current  $\hat{I}_0$  is completely determined by the shape of the column, i.e., by the reactive impedance  $Z_R$ . For Eq. (17), which determines the current  $\hat{I}_R$ , to be valid, the reactive impedance  $Z_R$  must be greater than the resistive impedance  $Z_a$ . According to (5.38)<sup>[1]</sup>, and taking into account the inductance of the filament, the reactive impedance in ohms is given by

$$Z_r = \frac{3.6 \cdot 10^{12}}{\omega l_0^2} \left( \ln \frac{2l_0}{b} - 1 \right) \left[ 1 - \left( \frac{4l_0}{\lambda_0} \right)^2 \right], \quad l \gg b. \quad (29)$$

Let us calculate the resistive impedance. The potential drop along the filament due to the skin resistance  $\rho_s$  will be

$$\hat{E}_0 = \frac{i}{l_0} \int_0^{l_0} \hat{I} \frac{\rho_s}{2\pi r} dz. \quad (30)$$

The quantity  $Z_a$  can be defined only somewhat arbitrarily. The current distribution along the filament depends on whether the reactance or resistance is larger. We will assume that the current distribution is determined by the reactance, and then, with (5.20) and (5.30) of <sup>[1]</sup>, we obtain

$$Z_a = \frac{\hat{E}_0}{\hat{I}_0} = i \frac{\rho_s}{2\pi l_0 b} \int_0^{l_0} \sqrt{1 - \frac{z^2}{l_0^2}} dz = \frac{i}{8b} \rho_s. \quad (31)$$

(We note here that in (5.39) of <sup>[1]</sup> we gave the impedance  $Z_a$  with an error in the numerator—instead of unity we wrote the letter  $l$ . The numerical coefficient is also not very accurate, as a result of the simplified derivation carried out in that article.) Replacing  $\rho_s$  by formula (5.33)<sup>[1]</sup> in the preceding equations, we obtain

$$Z_a = i \frac{2}{3l_0} R [\text{ohms}]. \quad (32)$$

As can be seen from Table II, for all powers  $Z_a$  is about a factor of ten smaller than  $Z_R$ . Under these conditions the current will be determined solely by the reactance with an accuracy better than 1%.

We can assume the reverse, that the current in the filament is determined by the resistive impedance  $Z_a$ , which under these conditions must be substantially greater than the reactance  $Z_R$ . These calculations are simple to carry out and lead to high values of the resistance  $R$ , and the skin resistance takes on a value  $\rho_s \approx 500$  ohms. This is ten times greater than the value for the cold plasma calculated from Eq. (6.6) of <sup>[1]</sup>.

The entire picture would be different from what we observe: for example, there would be no limitation of the filament length  $2l_0 \ll \lambda/2$ . It is possible that the diffuse form of discharge observed at low powers, which is the precursor of the filamentary discharge, arises just for

$$|Z_e| > |Z_r|.$$

As we have already indicated, for powers greater than 10 kW, the filament length is so close to  $\lambda/2$  that the determination of the current is already unreliable. For the limiting powers of 15 kW when the filament stops growing in length and only increases in diameter, the current will be determined mainly by the resistive impedance, and therefore determination of the current will require an accurate knowledge of the skin resistance and the radius in the hot region of the plasma, which up to the present time are inaccessible.

## 6. Conclusions

If we know the filament resistance  $R$ , the skin resistance  $\rho_S$  can be calculated from Eq. (5.33).<sup>[1]</sup> The quantity which can be determined with the least accuracy is radius  $b$  which defines the boundary of the region on whose surface the current flows in the filament. We can state with confidence that the radius  $b$  is appreciably smaller than the radius  $a_0$  based on (2.1)<sup>[1]</sup> which determines the external dimension of the luminous cloud surrounding the filament, so that we have the possibility of determining reliably only an upper limit  $\rho_m$  for the skin resistance. According to (5.33)<sup>[1]</sup> it will be given by

$$\rho_m = \frac{16 a_0}{3 l_0} R > \rho_s, \quad a_0 > b. \quad (33)$$

The value of  $\rho_m$  is listed in Table II.

It can be seen from Table II that for  $P_a = 8$  and 10 kW the skin resistance of the filament  $\rho_m$  will be respectively 2.9 and 1.3 ohms. On comparing these values of  $\rho_m$  with the value  $\rho_S$  calculated for the plasma at various temperatures (see Fig. 6.1<sup>[1]</sup>), we see that the limiting value  $\rho_m$  is less than the skin resistance  $\rho_S = 10$ –3 ohms for the cold plasma in the temperature range 6000–8000°, which is inadmissible. Here  $\rho_m$  is two to three times larger than the skin resistance of the hot plasma at  $T_e = 10^6$  degrees. If we take into account the uncertainty existing in determination of the dimensions of the hot plasma region and the approximate nature of the calculation of anomalous skin resistance, this is quite acceptable. Thus, the data obtained in measurement of  $\rho_m$  confirm the existence in the filament of a core with a hot plasma.

In<sup>[1]</sup> in Sec. 6 we calculated the pressure produced by the magnetic field (pinch) and the electric field on the plasma in the filament. According to (6.31)<sup>[1]</sup> the pressure  $p_H$  from the magnetic field produced by the current in the volume under the skin-layer of the filament will be

$$\bar{p}_H = \frac{\hat{I}_0^2}{2\pi b^2} \gg \frac{\hat{I}_0^2}{2\pi a_0^2} \quad \text{for } z = 0. \quad (34)$$

The radius  $b$  determines the hot plasma region where the current flows. We do not yet know how to determine

it, but in any case it is appreciably smaller than the external radius  $a_0$  of the cloud. At this stage we have the possibility of determining reliably only a lower limit for the pressure  $p_H$ . From the data of Table II for  $P_a = 10$  kW for  $\hat{I}_0 = 75$  A, and  $a_0 = 0.28$  cm, it will be 114 dynes/cm<sup>2</sup>.

The radius  $b$  is evaluated in<sup>[1]</sup> from Eq. (3.12); it is approximately a factor of two smaller than  $a_0$ , and therefore in reality the pressure will be  $p_H = 500$  dynes/cm<sup>2</sup>. This pressure is felt by the electrons in the skin layer and is transferred by collisions to the entire plasma located inside the region bounded by the radius  $b$ . This leads to the result that the partial pressure of the electrons increases, and the electron density rises correspondingly by an amount  $\Delta N_e$ , which is determined by Eq. (3.2)<sup>[1]</sup>:

$$\Delta N_e = \frac{p_H \cdot 10^{16}}{1.35 T_e} [\text{cm}^{-3}], \quad (35)$$

where  $p_H$  is in dynes/cm<sup>2</sup>.

If the plasma were cold with a temperature of about 7000°, then for  $p_H = 500$  dynes/cm<sup>2</sup> we would have  $\Delta N_e = 5 \times 10^{14}$ . This is several times greater than the electron density  $N_e$  calculated from (3.5)<sup>[1]</sup> and observed from the Stark broadening of the  $H_\beta$  line. It is necessary to take into account that the excess of electrons  $\Delta N_e$  diffusing into the filament will be decreased as the result of recombination. However, calculations show that this decrease is insufficient to explain the absence of broadening of the  $H_\beta$  lines with increasing current as the discharge power rises. From the curves of Fig. 3.2<sup>[1]</sup> it is evident that this is not observed, and the reverse occurs: the width of the lines decreases with increasing discharge power.

According to (35), in a hot plasma at  $T_e = 10^6$  degrees the density increase  $\Delta N_e$  will be smaller by about a factor of two and cannot produce a noticeable effect. This also confirms the existence of a hot plasma in the filament.

In the near future we hope to make more accurate measurements of the skin resistance, since in recent experiments it has become possible to determine the electron density distribution across the filament by illumination of the plasma filament by a microwave beam with a wavelength less than 1 mm.

In carrying out these experiments we have been grateful for the help given by engineers A. B. Manenkov, V. I. Chekin, N. I. Kondrat'ev, and A. V. Lebedev, electromechanician N. I. Milyukov, and designer N. V. Filimonov.

<sup>1</sup>P. L. Kapitza, Zh. Eksp. Teor. Fiz. 57, 1801 (1969) [Sov. Phys.-JETP 30, 973 (1970)].

<sup>2</sup>P. L. Kapitza, Zh. Eksp. Teor. Fiz. 58, 377 (1970) [Sov. Phys.-JETP 31, 199 (1970)].

<sup>3</sup>P. L. Kapitza, S. I. Filimonov, and S. P. Kapitza, Élektronika bol'shikh moshchnostey (High Power Electronics) 3, Nauka, 1969, p. 7.

<sup>4</sup>P. L. Kapitza, S. I. Filimonov, and S. P. Kapitza, Élektronika bol'shikh moshchnostey (High Power Electronics) 6, Nauka, 1969, p. 7.

<sup>5</sup>P. L. Kapitza, Élektronika bol'shikh moshchnostey

(High Power Electronics) 4, Nauka, 1965, p. 7.

<sup>6</sup> P. L. Kapitza and L. A. Prozorova, *Elektronika bol'shikh moshchnostey* (High Power Electronics) 4, Nauka, 1965, p. 53.

<sup>7</sup> P. L. Kapitza and S. I. Filimonov, *Elektronika bol'shikh moshchnostey* (High Power Electronics) 6, Nauka, 1969, p. 147.

<sup>8</sup> P. L. Kapitza, *Elektronika bol'shikh moshchnostey* (High Power Electronics) 4, Nauka, 1965, p. 206.

<sup>9</sup> S. Ramo and J. R. Whinnery, *Fields and Waves in Modern Radio*, Wiley, New York, 1953, VI ed., p. 555.

Translated by C. S. Robinson

103